

Analyst

Accepted Manuscript



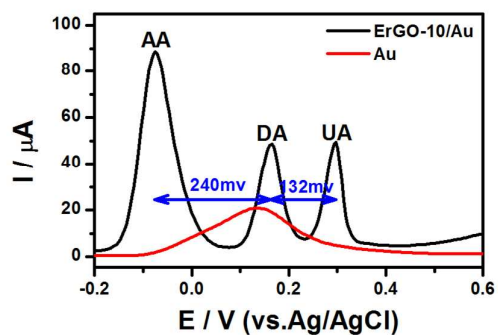
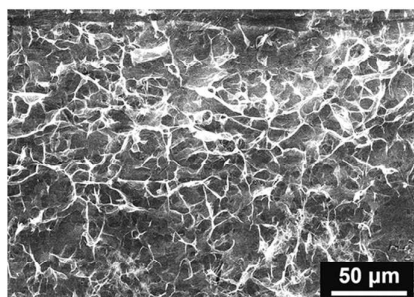
This is an *Accepted Manuscript*, which has been through the Royal Society of Chemistry peer review process and has been accepted for publication.

Accepted Manuscripts are published online shortly after acceptance, before technical editing, formatting and proof reading. Using this free service, authors can make their results available to the community, in citable form, before we publish the edited article. We will replace this *Accepted Manuscript* with the edited and formatted *Advance Article* as soon as it is available.

You can find more information about *Accepted Manuscripts* in the [Information for Authors](#).

Please note that technical editing may introduce minor changes to the text and/or graphics, which may alter content. The journal's standard [Terms & Conditions](#) and the [Ethical guidelines](#) still apply. In no event shall the Royal Society of Chemistry be held responsible for any errors or omissions in this *Accepted Manuscript* or any consequences arising from the use of any information it contains.

Graphical abstract



A three-dimensional (3D) interpenetrating electrode of reduced graphene oxide with high electrocatalytic activity was fabricated by one-step electrodeposition for selective detection of dopamine.

Three-dimensional interpenetrating electrode of reduced graphene oxide for selective detection of dopamine†

Cite this: DOI: 10.1039/x0xx00000x

Xiaowen Yu, Kaixuan Sheng and Gaoquan Shi*

Received 00th January 2012,
Accepted 00th January 2012

DOI: 10.1039/x0xx00000x

www.rsc.org/

Electrochemical detection of dopamine plays an important role in medical diagnosis. In this paper, we report a three-dimensional (3D) interpenetrating graphene electrode fabricated by electrochemical reduction of graphene oxide for selective detection of dopamine. This electrochemically reduced graphene oxide (ErGO) electrode was used directly without further functionalization or blending with other functional materials. This electrode can efficiently lower the oxidation potential of ascorbic acid; thus, it is able to selectively detect dopamine in the presence of ascorbic acid and uric acid. The ErGO-based biosensor exhibited a linear response towards dopamine in the concentration range of 0.1–10 μM with a low detection limit of 0.1 μM . Furthermore, this electrode has good reproducibility and environmental stability, and can be used to analyse real samples.

1. Introduction

3,4-Dihydroxyphenylethylamine, dopamine (DA), is one of the important neurotransmitters, playing a significant role in the function of human metabolism, cardiovascular, central nervous, renal, and hormonal systems.^{1,2} Abnormal levels of DA in body fluids are the indications of many serious diseases such as Schizophrenia, Huntington's and Parkinson's diseases.³ Electrochemical methods have been extensively explored for the detection of DA because of their simple processes and cheap instruments.⁴ However, the major challenge of sensing DA in real samples is the coexistence of high concentrations of ascorbic acid (AA) and uric acid (UA) with oxidation potentials close to that of DA at conventional electrodes, offering strong interferences.^{5,6}

On the other hand, graphene materials have been widely applied for the fabrication of electrochemical sensors because of their unique atom-thick two-dimensional structures, high conductivity and electrocatalytic activities, large specific surface areas and excellent electrochemical stability.^{7–15} However, in these cases, graphene sheets were usually coated on the surfaces of substrate electrodes as compact films. As a result, the inherent properties of individual graphene sheets cannot be inherited to the buck graphene coatings.¹⁶ To address this problem, many attempts have been made to construct three-dimensional (3D) graphene architectures.^{16–18} These 3D architectures provide graphene materials with high specific surface areas, strong mechanical strengths and fast mass and

electron transport kinetics because of the combination of 3D porous structures and the excellent intrinsic properties of graphene.¹⁷ One of the most widely used 3D porous graphene materials used for electrochemical sensing was prepared by chemical vapour deposition (CVD) of graphene sheets onto nickel foams.¹⁸ The CVD method can produce high-quality graphene with excellent electrical conductivity,¹⁹ while it suffers from high cost and complicated process. Furthermore, the CVD-graphene has a low content of oxygenated species and structural defects, making its electrocatalytic activity is much weaker than that of edge plane pyrolytic graphite (EPPG).²⁰ This is mainly due to that the oxygenated groups and absorption sites of carbon-based electrodes are important for catalyzing the electrochemical reactions of many analytes.^{21, 22} Electrochemical deposition is a green, facile, and low cost approach to prepare electroactive materials on the surfaces of electrodes, and the modified electrodes can be directly used in electrochemical devices.¹⁷ Here, we report an ErGO electrode with a 3D interpenetrating microstructure for electrochemically sensing DA. This electrode showed an excellent performance towards DA with remarkable selectivity and reproducibility, good stability, and a low detection limit of 0.1 μM .

2. Experimental

2.1. Chemicals

Natural graphite powder (325 mesh) was obtained from Qingdao Huatai lubricant sealing S&T Co. Ltd. (Qingdao,

China). Uric acid, dopamine hydrochloride, and ascorbic acid were purchased from Alfa Aesar. Human serum purchased from BioDee Company (Beijing, China). All other reagents, including H_2SO_4 , HCl , H_2O_2 (30 wt %), KMnO_4 , NaNO_3 , LiClO_4 , $\text{K}_3\text{Fe}(\text{CN})_6$, $\text{K}_4\text{Fe}(\text{CN})_6$, K_2HPO_4 and $\text{KH}_2\text{PO}_4 \cdot 3\text{H}_2\text{O}$ were of analytical pure grade and bought from the Beijing Chemical Reagent Company (Beijing, China). All chemicals were used as received without further purification. The aqueous solutions were prepared using double distilled water. The 0.1 M phosphate buffer solution (PBS, pH = 7.0) was prepared from K_2HPO_4 and $\text{KH}_2\text{PO}_4 \cdot 3\text{H}_2\text{O}$.

Graphene oxide (GO) was synthesized from natural graphite powder by a modified Hummers method,²³ and it was purified by dialysis for one week to remove the remaining metal species. Finally it was centrifuged at 4000 rpm to remove the incompletely oxidized graphite powder.

2.2. Preparation of electrodes

ErGO electrodes were fabricated by electrochemical deposition of rGO sheets on the surface of Au electrodes. Prior to use, Au electrodes (3 mm diameter) were carefully polished with 0.5 and 0.05 μm alumina powder slurries, then washed by sonication successively in water and ethanol for a few minutes. The clean Au electrode was used as the working electrode, a platinum (Pt) foil was applied as the counter electrode and all the potentials were referred to a saturated calomel electrode (SCE). A 6 mg mL^{-1} GO dispersion containing 0.2 M LiClO_4 was used as the electrolyte. The electrochemical deposition was carried out at a constant potential of -1.2 V by using a CHI 660D potentiostat-galvanostat (CH Instruments Inc.). During this process, GO sheets were reduced into conductive ErGO as reported in the literature.²⁴⁻²⁶ Finally, the ErGO electrodes were

washed and immersed in deionized water for 1 h to remove the residual GO absorbed on the electrodes. Before using the ErGO electrodes, they should be immersed in water to maintain their morphology.

2.3. Characterizations

The morphology of ErGO electrode was studied by using a field-emission scanning electron microscope (Sirion-200, Japan). Raman spectra were recorded on a Renishaw Raman microscope with a 514-nm laser. X-ray photoelectron spectra (XPS) were taken out by using an ESCALAB 250 photoelectron spectrometer (ThermoFisher Scientific, USA) with $\text{Al K}\alpha$ (1486.6 eV) as the X-ray source set at 200 W and a pass energy of 30 eV for high resolution scan. The electrochemical tests were performed on a CHI 660D potentiostat-galvanostat (CH Instruments Inc.) at room temperature. The ErGO electrode, Pt gauze, and an Ag/AgCl electrode were used as the working, counter, and reference electrodes, respectively. All of the solutions were deoxygenated by bubbling nitrogen gas for 15 min before electrochemical measurements. For chronocoulometry studies, the initial potential was 0.65 V and the potential was stepped to -0.05 V. The electrochemical impedance spectra were taken out in the frequency range of 0.1 Hz to 100 kHz with 5 mV ac amplitude.

3. Results and discussion

3.1. Characterization of ErGO electrodes

The ErGO electrodes were prepared by electrochemical reduction of 6 mg mL^{-1} GO for 5, 10, 20 or 40 s, and they are nominated as ErGO-t, where t is the time of electrodeposition

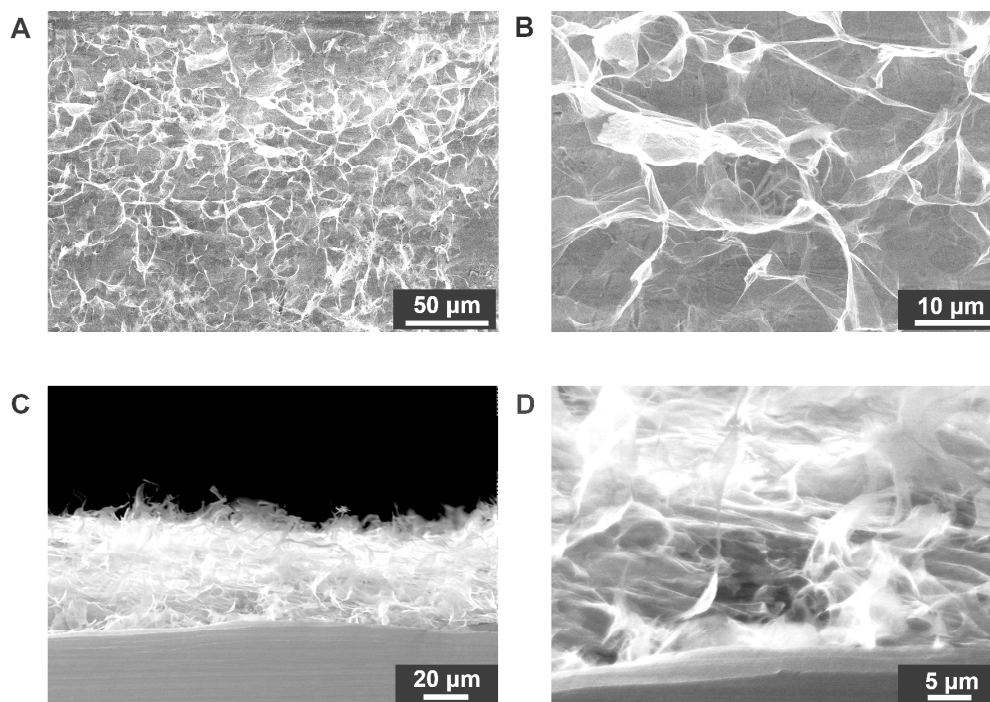


Fig. 1 (A, B) top view and (C, D) cross-sectional scanning electron microscope images of ErGO-10 deposited on Au substrate electrode with different magnifications.

in second. Here, we take ErGO-10 (Fig. S1†) as an example for morphological and structural studies, and its SEM images are shown in Fig. 1. The ErGO sheets generated by electrochemical reduction have more conjugated domains and less oxygenated groups than those of their GO precursor. As a result, upon the driving of electric field, they were self-assembled to form a 3D interpenetrating network (Fig. 1A, B) with a thickness of about 30 μm (Fig. 1C) because of hydrophobic and π -stacking interactions.²⁷ Furthermore, the residual hydrophilic oxygenated groups of ErGO sheets made the pores of 3D network were filled with aqueous electrolyte. The pore sizes of the network are in the range of several micrometers to larger than ten micrometers. The pore walls consist of thin layers of stacked graphene sheets, providing physical cross-linking sites to stabilize the interpenetrating 3D network.²⁷ The pore walls are nearly vertical to the surface of Au electrode (Fig. 1B, C, and D), therefore, the micropores in the electrode fully expose to the electrolyte for the access of ions and target molecules. Moreover, the upright oriented graphene sheets provide more graphene edges as active sites for electrocatalysis.^{28–32}

The Raman spectrum of GO or ErGO-10 (Fig. 2A) has two prominent bands around 1340 and 1580 cm^{-1} , and they are assigned to the D- and G-bands of carbon, respectively. The D-band is associated with the structural defects or partially disordered structures of graphite domains and the G-band is related to graphitic carbon.³³ The intensity ratio of D- and G-bands (I_D/I_G) of GO was calculated to be 0.72, while that of ErGO-10 was increased to 1.28. This result indicates that the oxidized areas of GO sheets were partly restored upon reduction to form small conjugated domains.³⁴

The C 1s XPS spectra of GO and ErGO-10 (Fig. 2B) indicate the presence of 4 types of carbon bonds: C-C/C=C (284.6 eV), C-O (286.6 eV), C=O (287.8 eV), and O-C=O (289.0 eV).²⁷ However, in the spectrum of ErGO-10, the bands associated with the oxygenated groups are much weaker than those in the spectrum of GO. The C/O atomic ratio of GO was measured to be 2.27, and that of ErGO-10 was increased to 3.14. These results also confirm that the oxygenated functional groups of GO were partially removed after electrochemical reduction.

3.2. Effects of electrodeposition time on ErGO electrodes

The morphology and electrochemical performances of ErGO electrodes can be modulated by controlling the time of electrodeposition. With increasing the deposition time from 5 to 40 s, the thickness of ErGO interpenetrating layer increased from about 10 to approximately 50 μm (Fig. 1, Fig. S2†). The cyclic voltammograms (CVs) of the ErGO electrodes in pure PBS are rectangular in shapes and the areas of the rectangles increased with the thickness of graphene layer (Fig. S3A†). Accordingly, the ErGO electrodes exhibited electrochemical double layer behavior and their areal specific capacitances increased with the increase of electrodeposition time.²⁵ The performances of the ErGO electrodes toward 10 μM DA in PBS were studied by differential pulse voltammetry (DPV). The ErGO electrode prepared by the electrochemical deposition for 10 s (ErGO-10) showed the strongest electrochemical response

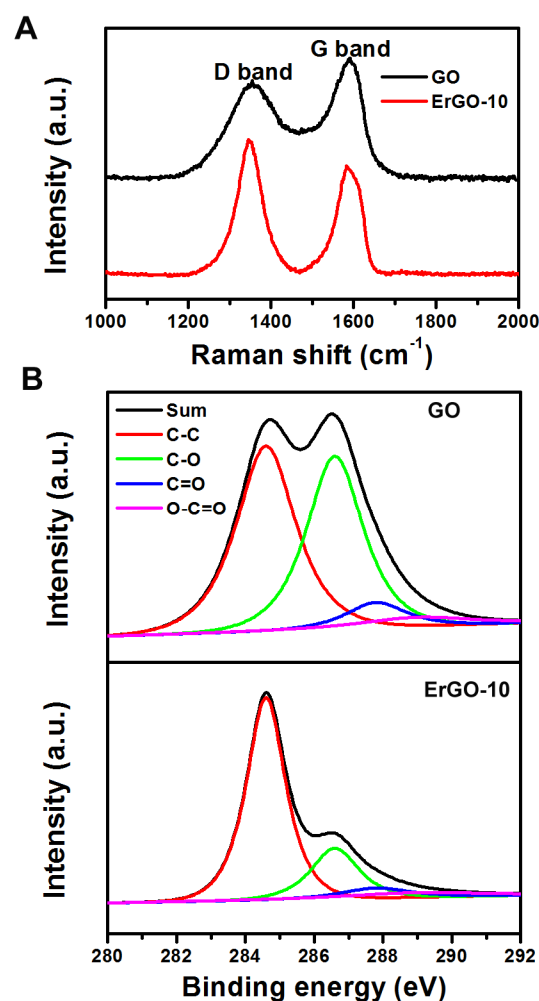


Fig. 2 (A) 514.5-nm excited Raman and (B) C 1s XPS spectra of GO and ErGO-10.

(Fig. S3B† and S3C†). This is possibly due to its optimized microstructure for electrocatalysis. As the electrochemical deposition time was short (e.g. ErGO-5), most graphene sheets laid parallel to the surface of substrate electrode to form a compact film. However, with the increase in deposition time (e.g. ErGO-20 and ErGO-40), the walls of graphene micropores became thicker comparing with those of ErGO-10 because of the stacking of graphene sheets. Furthermore, the thickness increase of the graphene layer also increased the distances of charge transfer and ion diffusion. Thus, we chose ErGO-10 electrode for the detection of DA.

3.3. Electrochemical behavior of ErGO-10 electrode

Potassium ferricyanide solution was used to evaluate the electrochemical behavior of ErGO-10 electrode. Fig. 3A shows the chronocoulometric curve of an ErGO-10 or an Au electrode for the reduction of 1 mM $\text{K}_3\text{Fe}(\text{CN})_6$ in the aqueous solution of 2 M KCl. The effective surface areas of both electrodes were calculated by the use of following equation.^{35, 36}

$$Q = (2nFAD_0^{1/2}\pi^{-1/2}C_0) t^{1/2}$$

Where Q is the absolute value of the reduction charge, n is the number of electrons for the reaction (ferricyanide, $n=1$), F is Faraday constant (96485 C mol^{-1}). A is the surface area of the electrode, D_0 is the diffusion coefficient of the oxidized form (ferricyanide, $D_0 = 7.6 \times 10^{-6} \text{ cm}^2 \text{ s}^{-1}$). C_0 is the bulk concentration of the oxidized form (1 mM), and t is the time. According to the slope of the linear plot of Q versus $t^{1/2}$, the electrochemically active surface area of Au electrode was calculated to be 0.070 cm^2 , and this value is in consistent with its geometry surface area (0.071 cm^2). The chronocoulometric curve of ErGO-10 electrode starts at a high charge value because of the high electric double layer capacitance of the electrode, and bends at the initial region caused by the surface adsorption of oxidized species.³⁵ According to the slope of the linear region of this curve, the electrochemically active surface area of ErGO-10 electrode was measured to be about twice that of Au electrode (0.133 cm^2), indicating its improved ability on electrochemical reaction.^{36, 37}

The capability of electron transfer of ErGO-10 or Au electrode was further investigated by AC impedance analysis (Fig. 3B). The Nyquist plot of bare Au electrode exhibits a semicircle with a charge-transfer resistance (R_{ct}) of about 212Ω . In comparison, the spectrum of ErGO-10 electrode is nearly a straight line with a negligible R_{ct} . This is mainly due to the opened porous microstructure of ErGO-10 electrode makes nearly all of the graphene sheets are accessible to electrolyte, facilitating the transfer of electrons and the diffusion of ions during the process of electrochemical reaction.

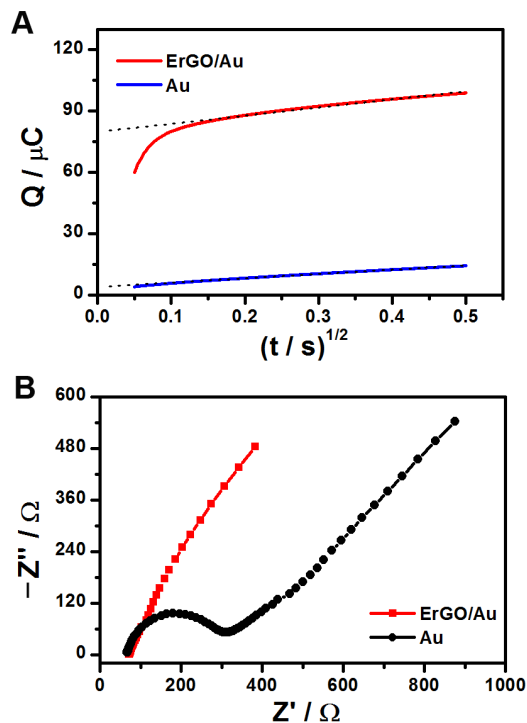


Fig. 3 (A) Chronocoulometric curve for the reduction of 1 mM $\text{K}_3\text{Fe}(\text{CN})_6$ in 2 M KCl at ErGO-10 or Au electrode; (B) Nyquist plots of ErGO-10 and Au electrodes in 5 mM $\text{Fe}(\text{CN})_6^{3-/4-}$ containing 0.1 M KCl.

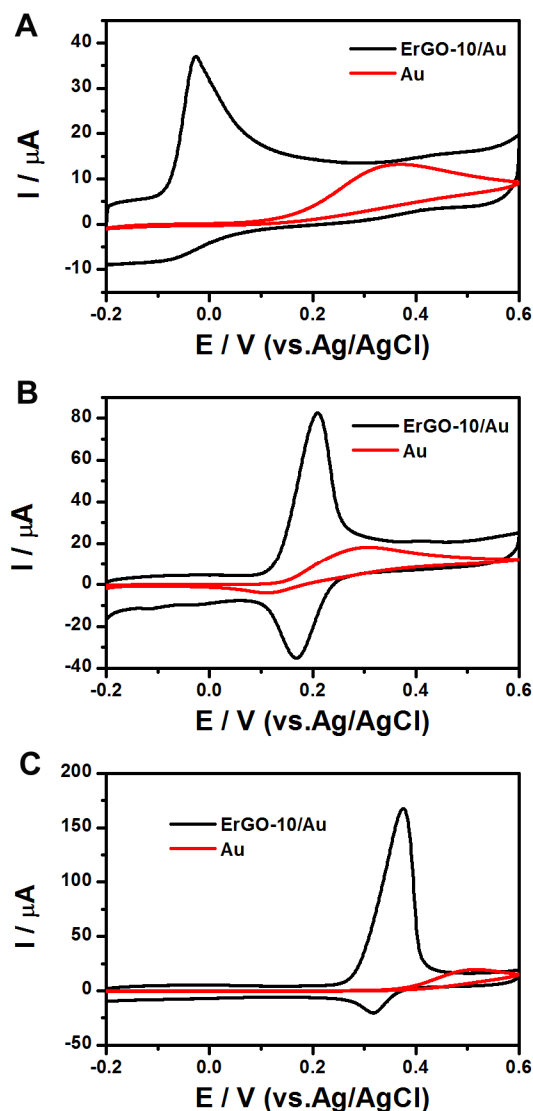


Fig. 4 CVs of 1 mM AA (A), DA (B), and UA (C) at ErGO-10 or Au electrode. Electrolyte = 0.1 M pH 7.0 PBS; Scan rate = 50 mV s^{-1} .

3.4. Electrochemical behaviors of AA, DA, and UA at ErGO-10 or Au electrode

Fig. 4 illustrates the CVs of 1 mM AA, DA, or UA at ErGO-10 or Au electrode. The CV of AA at a bare Au electrode shows only a broad oxidation wave centered at $+0.367 \text{ V}$ (Fig. 4A). However, at ErGO-10 electrode, this wave was negatively shifted for 0.393 V to be centered at around -0.026 V . The negative shift of the peak potential of AA is especially crucial to the separation of three analytes.³⁸ The CV of DA at ErGO-10 electrode has a couple of redox waves and the potential difference of their peaks (ΔE_p) was measured to be only 0.043 V , whereas the ΔE_p in the CV at Au electrode was calculated to be as large as 0.196 V (Fig. 4B). The anodic wave potential at ErGO-10 electrode is about $+0.210 \text{ V}$, lower than that at Au electrode. In the case of UA (Fig. 4C), a couple of redox waves with a ΔE_p of 0.058 V are observed from the CV at ErGO-10 electrode. The peak potential of the oxidation wave was

measured to be +0.375 V and this value is 0.152 V lower than that observed at Au electrode (+0.517 V). Furthermore, the current densities of the oxidation waves of AA, DA, and UA at ErGO-10 electrode are about 2, 6, and 15 times those at Au electrode, respectively. The large negative shifts of the anodic wave potentials together with the strong enhancements in redox currents and the decrease in ΔE_p indicate the excellent electrocatalytic activity and fast electron transport kinetics at ErGO-10 electrode.^{39, 40} The superior performance of ErGO-10 electrode is attributed to its large electrochemically active area and negligible R_{ct} (Fig. 3) as well as its multiplexed and highly conductive pathways provided by the 3D interpenetrating graphene network.^{16, 41} Furthermore, the exposed edges of ErGO sheets are favourable sites for transferring electrons from electrode to biomolecules.^{30, 31, 37, 42} In order to demonstrate that the 3D architecture of ErGO-10 electrode plays a key role in their electrochemical performances, we dried this electrode in air. As a result, the 3D microstructure of ErGO was collapsed to form a compact 2D film because of the volume contraction of graphene layer and π -stacking of graphene sheets during the process of drying (Fig. S4†). The DPV curve of 1 mM DA at the compact 2D graphene electrode showed an oxidation current density about 3 times weaker than that at the untreated ErGO-10 electrode (Fig. S5†). This is mainly due to the compact 2D ErGO film has much smaller surface area for the access of electrolyte and DA molecules and fewer exposed graphene edges for electrocatalysis.

3.5. Simultaneous detection of AA, DA, and UA

AA, DA, and UA coexist in serum and other extracellular body fluids and their selective determination in a ternary mixture is of great importance in biosensing. For this purpose, a mixture of 5 mM AA, 0.1 mM DA, and 0.1 mM UA was used as the sensing sample. The CV of this mixture at Au electrode shows only a broad oxidation wave in the potential range of 0.1 to 0.6 V because of the wave overlapping of the three analytes (Fig. 5A). In comparison, at ErGO-10 electrode, the CV shows three well-defined peaks at approximately -0.013 (AA), +0.197 (DA) and +0.336 V (UA), respectively. The peak potential separations between neighboring waves were measured to be 0.210 V (AA and DA) and 0.139 V (DA and UA). Accordingly, the ErGO-10 electrode can provide much larger voltammetric peak separations than those of Au electrode; thus, it can efficiently detect one species in the presence of other two coexist analytes. The selectivity of our ErGO-10 electrode is superior to that of the electrode based on multilayer graphene nanoflakes³² or functionalized graphene.⁴³ It should be noted here, the reduction waves of these three analytes are also shown in the CV curve of ErGO-10 electrode, reflecting the ultrahigh electrocatalytic activity of this electrode. In addition, the ErGO-10 electrode can also discriminate these three species even at a fast scan rate of 1000 mV s⁻¹ (Fig. S6†). This is possibly due to the high efficiency of electron transfer between the molecules of analytes and the 3D interpenetrating graphene network of ErGO-10 electrode.

DPV analysis also exhibited an excellent performance in simultaneous determination of AA, DA, and UA without any interferences. As shown in Fig. 5B, the oxidation peaks of 5 mM AA, 0.1 mM DA, and 0.1 mM UA at ErGO-10 electrode

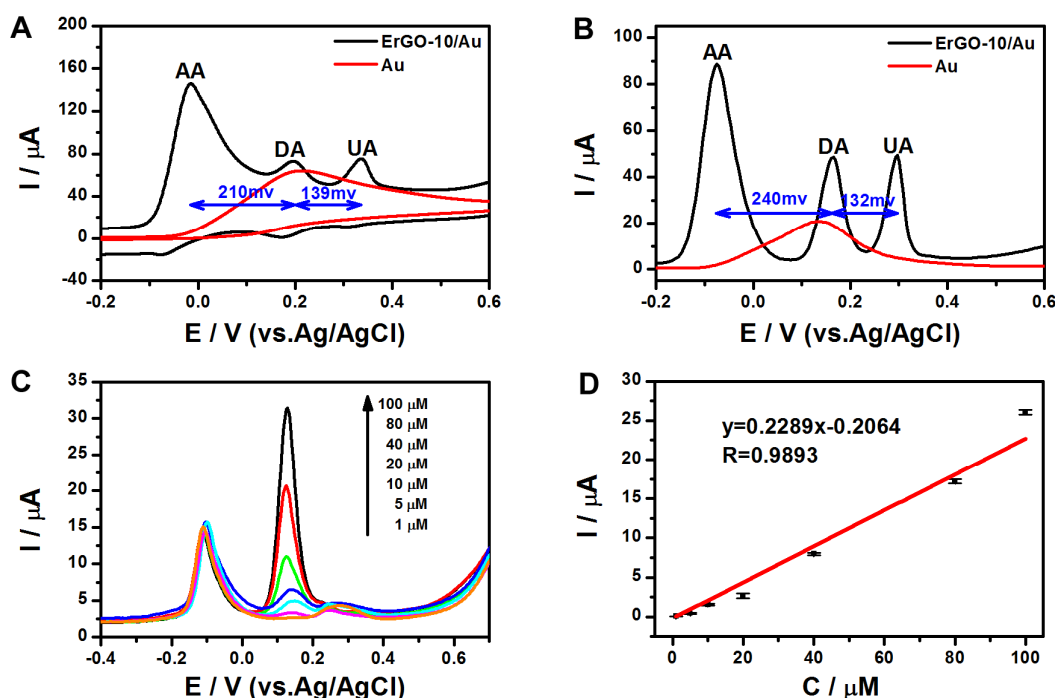


Fig. 5 (A) CVs (scan rate: 50 mV s⁻¹) and (B) DPVs (pulse width: 0.2 s; pulse period: 0.5 s) of a mixed solution containing 5 mM AA, 0.1 mM DA, and 0.1 mM UA at ErGO-10 or Au electrode. (C) DPVs of a 0.1 M pH 7.0 PBS solution containing 500 μM AA, 10 μM UA and different concentrations of DA at ErGO-10 electrode. (D) Linear fit of peak currents to concentrations of DA according to the curves shown in panel C.

are centered at -0.076 , $+0.164$, and $+0.296$ V, respectively. The potential separations among the peaks are 0.240 (AA and DA), 0.132 (DA and UA), and 0.372 V (AA and UA), larger than the values achieved at a chitosan-graphene modified electrode (correspondingly, 0.165 , 0.090 , and 0.255 V).⁴⁴ These results also reflect that ErGO-10 electrode can be used for simultaneous sensing these three species in a mixture. It should be noted here, ErGO-10 was used directly without further functionalization or blending with other functional materials.

Fig. 5C illustrates the DPV curves of DA with different concentrations at ErGO-10 electrode in the presence of 500 μM AA and 10 μM UA. The peak current of DPV curve increases linearly with the concentration of DA in the range of 1 to 100 μM (Fig. 5D), indicating that the interferences of AA and UA are negligible.

3.6. Amperometric response of DA

The amperometric responses of ErGO-10 electrode towards DA at $+0.200$ V are demonstrated in Fig. 6. Fig. 6A is an amperometric current-time plot and the limit of detection was tested to be as low as 0.1 μM ($S/N=3$), the corresponding calibration curve is inserted in this figure. This value is lower than those reported previously for the graphene modified electrodes (≥ 0.5 μM).⁴³⁻⁴⁷ In Fig. 6B, the linear relationship between the peak currents and DA concentrations was obtained for the DA range of $0.1\sim 10$ μM . The linear regression equation is I (μA) = 0.0443 C (μM), with a correlation coefficient of $R=0.9996$ ($N=3$), where I and C are the current of response and the concentration of DA.

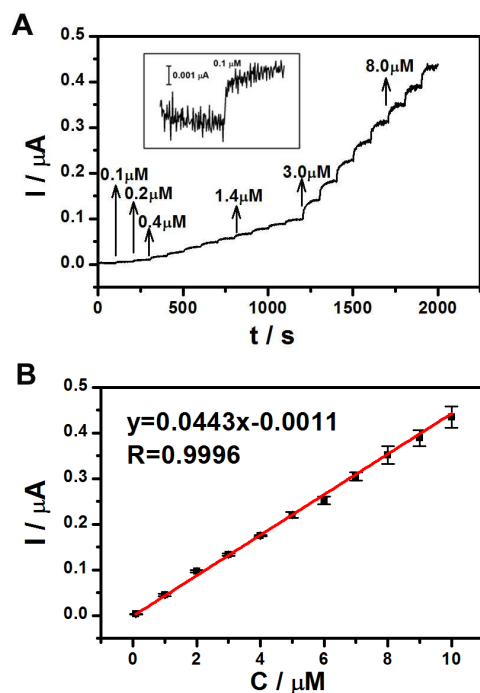


Fig. 6 (A) Amperometric responses of the ErGO-10 electrode at 0.200 V after the subsequent addition of DA in a 0.1 M PBS (pH 7.0) solution; inset is the corresponding calibration curve of 0.1 μM DA. (B) Linear fit of peak currents to the concentrations of DA.

3.7. Reproducibility and stability of ErGO-10 electrode

The reproducibility of ErGO-10 electrode was investigated by using 6 electrodes prepared under the identical conditions, and the relative standard deviation (RSD) of their electrochemical responses to 1 mM DA was measured to be only 1.4% (Fig. S7 \dagger). The amperometric response remained 88% of its initial value after immersing for $1,500$ s in the solution of 50 μM DA under stirring (Fig. S8 \dagger). The ErGO-10 electrode also showed excellent environmental stability; it kept about 90% of its initial current signal after storing in PBS at 4 $^{\circ}\text{C}$ for 1 week (Fig. S9 \dagger).

3.8. Real sample analysis

The detection of DA in human serum was also performed to clarify whether the ErGO-10 electrode can be practically applied for analyzing real samples. For this purpose, human serum was first centrifuged at 4000 rpm for 20 min to obtain a transparent liquid outside the ultrafiltration membrane (molecular weight cut off = 5 kDa). Then, the purified serum was diluted for ten times (by volume) with PBS. Diluted human serum containing 10 μM DA was measured by DPV with ErGO-10 electrode and the measurements were repeated for 5 times (Fig. S10 \dagger). The found values were calculated by referring to the standard curve shown in Fig. 5D (Table 1). Accordingly, the average recovery was calculated to be 99.70% with a relative standard derivation of only 2.22% . These results reflect that the substrates in serum (e. g. AA, UA, proteins, amino acids) do not interfere the detection of DA, suggesting the ErGO-10 electrode can be applied for analyzing real samples.

Table 1 Electrochemical detection of 10 μM DA in human serum for 5 times with ErGO-10 electrodes.

Sample	Found (μM)	Recovery (%)
1	9.94	99.4
2	9.71	97.1
3	10.17	101.7
4	10.22	102.2
5	9.81	98.1

4. Conclusions

We developed a one-step electrochemical method to fabricate 3D interpenetrating ErGO electrode for electrochemical sensing. This method, analogous to electroplating process, can be carried out in an aqueous medium and does not need expensive equipment like CVD technique or a toxic reducing agent frequently required by chemical reduction of GO. Therefore, it is fast, simple, cheap, eco-friendly, easy controllable, and readily scalable to industrial levels. Furthermore, the microporous 3D ErGO electrode has high electrochemical performance because of its large accessible surface area, highly conductive channels and strong electrocatalytic activity. Therefore, it can be used to selectively detect DA with an extremely low limit of detection compared with other graphene electrodes. The ErGO electrode can be used directly without further modification or blending with other functional materials. The 3D interpenetrating ErGO electrode provides a promising and attractive platform for

fabricating electrochemical biosensors with good selectivity, sensitivity, reproducibility, and stability.

Acknowledgements

This work was supported by the National Basic Research Program of China (2012CB933402) and the National Natural Science Foundation of China (51161120361, 21274074).

Notes and references

Department of Chemistry, Tsinghua University, Beijing 100084, People's Republic of China.

E-mail: gshi@tsinghua.edu.cn

Tel: +86-10-62773743; Fax: +86-10-62771149

†Electronic Supplementary Information (ESI) available: [Supplementary figures about the electrodes prepared under different conditions, the repeatability and stability of the electrodes]. See DOI: 10.1039/b000000x/

- 1 J. F. van Staden and R. I. van Staden, *Talanta*, 2012, **102**, 34.
- 2 M. L. Heien, A. S. Khan, J. L. Ariansen, J. F. Cheer, P. E. Phillips, K. M. Wassum and R. M. Wightman, *Proc. Natl. Acad. Sci. U.S.A.*, 2005, **102**, 10023.
- 3 R. M. Wightman, L. J. May and A. C. Michael, *Anal. Chem.*, 1988, **60**, 769A.
- 4 P. Quan do, P. Tuyen do, T. D. Lam, P. T. Tram, N. H. Binh and P. H. Viet, *Colloids Surf. B*, 2011, **88**, 764.
- 5 C. Deng, J. Chen, M. Wang, C. Xiao, Z. Nie and S. Yao, *Biosens. Bioelectron.*, 2009, **24**, 2091.
- 6 M. Bagherzadeh and M. Heydari, *Analyst*, 2013, **138**, 6044.
- 7 A. K. Geim and K. S. Novoselov, *Nat. Mater.*, 2007, **6**, 183.
- 8 R. M. Westervelt, *Science*, 2008, **320**, 324.
- 9 D. A. C. Brownson and C. E. Banks, *Analyst*, 2010, **135**, 2768.
- 10 Y. Liu, X. Dong and P. Chen, *Chem. Soc. Rev.*, 2012, **41**, 2283.
- 11 C. Huang, C. Li and G. Shi, *Energy Environ. Sci.*, 2012, **5**, 8848.
- 12 D. Chen, L. Tang and J. Li, *Chem. Soc. Rev.*, 2010, **39**, 3157.
- 13 S. Alwarappan, A. Erdem, C. Liu and C.-Z. Li, *J. Phys. Chem. C*, 2009, **113**, 8853.
- 14 S. Alwarappan, C. Liu, A. Kumar and C.-Z. Li, *J. Phys. Chem. C*, 2010, **114**, 12920.
- 15 M. Mishra, S. Alwarappan, R. K. Joshi and T. Mohanty, *J. Nanosci. Nanotechnol.*, 2013, **13**, 4040.
- 16 X. Dong, X. Wang, L. Wang, H. Song, H. Zhang, W. Huang and P. Chen, *ACS Appl. Mater. Interfaces*, 2012, **4**, 3129.
- 17 C. Li and G. Shi, *Nanoscale*, 2012, **4**, 5549.
- 18 D. A. C. Brownson, L. C. S. Figueiredo-Filho, X. Ji, M. Gomez-Mingot, J. Iniesta, O. Fatibello-Filho, D. K. Kampouris and C. E. Banks, *J. Mater. Chem. A*, 2013, **1**, 5962.
- 19 X. Cao, Y. Shi, W. Shi, G. Lu, X. Huang, Q. Yan, Q. Zhang and H. Zhang, *Small*, 2011, **7**, 3163.
- 20 D. A. C. Brownson, M. Gomez-Mingot and C. E. Banks, *Phys. Chem. Chem. Phys.*, 2011, **13**, 20284.
- 21 D. A. C. Brownson, R. V. Gorbachev, S. J. Haigh and C. E. Banks, *Analyst*, 2012, **137**, 833.
- 22 D. A. C. Brownson, C. W. Foster and C. E. Banks, *Analyst*, 2012, **137**, 1815.
- 23 W. S. Hummers and R. E. Offeman, *J. Am. Chem. Soc.*, 1958, **80**, 1339.
- 24 M. Hilder, B. Winther-Jensen, D. Li, M. Forsyth and D. R. MacFarlane, *Phys. Chem. Chem. Phys.*, 2011, **13**, 9187.
- 25 K. Sheng, Y. Sun, C. Li, W. Yuan and G. Shi, *Sci. Rep.*, 2012, **2**, 247.
- 26 Y. Li, K. Sheng, W. Yuan and G. Shi, *Chem. Commun.*, 2013, **49**, 291.
- 27 Y. Xu, K. Sheng, C. Li and G. Shi, *ACS Nano*, 2010, **4**, 4324.
- 28 C. Gómez-Navarro, J. C. Meyer, R. S. Sundaram, A. Chuvilin, S. Kurasch, M. Burghard, K. Kern and U. Kaiser, *Nano Lett.*, 2010, **10**, 1144.
- 29 K. Erickson, R. Erni, Z. Lee, N. Alem, W. Gannett and A. Zettl, *Adv. Mater.*, 2010, **22**, 4467.
- 30 C. E. Banks and R. G. Compton, *Analyst*, 2005, **130**, 1232.
- 31 C. E. Banks, T. J. Davies, G. G. Wildgoose and R. G. Compton, *Chem. Commun.*, 2005, 829.
- 32 N. G. Shang, P. Papakonstantinou, M. McMullan, M. Chu, A. Stamboulis, A. Potenza, S. S. Dhesi and H. Marchetto, *Adv. Funct. Mater.*, 2008, **18**, 3506.
- 33 K. N. Kudin, B. Ozbas, H. C. Schniepp, R. K. Prud'homme, I. A. Aksay and R. Car, *Nano Lett.*, 2008, **8**, 36.
- 34 A. C. Ferrari and J. Robertson, *Phys. Rev. B*, 2000, **61**, 14095.
- 35 Bard, A. J.; Faulkner, L. R. *Electrochemical Methods, Fundamentals and Applications*, 2nd ed.; John Wiley and Sons: Beijing, 2005.
- 36 M. Csizsar, A. Szucs, M. Tolgyesi, A. Mechler, J. B. Nagy and M. Novak, *J. Electroanal. Chem.*, 2001, **497**, 69.
- 37 M. Zhou, Y. Zhai and S. Dong, *Anal. Chem.*, 2009, **81**, 5603.
- 38 C.-L. Sun, H.-H. Lee, J.-M. Yang and C.-C. Wu, *Biosens. Bioelectron.*, 2011, **26**, 3450.
- 39 Y. Guo, S. Guo, J. Ren, Y. Zhai, S. Dong and E. Wang, *ACS Nano*, 2010, **4**, 4001.
- 40 C.-L. Sun, C.-T. Chang, H.-H. Lee, J. Zhou, J. Wang, T.-K. Sham and W.-F. Pong, *ACS Nano*, 2011, **5**, 7788.
- 41 R. S. Kelly, D. J. Weiss, S. H. Chong and T. Kuwana, *Anal. Chem.*, 1999, **71**, 413.
- 42 W. Yuan, Y. Zhou, Y. Li, C. Li, H. Peng, J. Zhang, Z. Liu, L. Dai and G. Shi, *Sci. Rep.*, 2013, **3**, 2248.
- 43 M. Mallesha, R. Manjunatha, C. Nethravathi, G. S. Suresh, M. Rajamathi, J. S. Melo and T. V. Venkatesha, *Bioelectrochem.*, 2011, **81**, 104.
- 44 D. Han, T. Han, C. Shan, A. Ivaska and L. Niu, *Electroanal.*, 2010, **22**, 2001.
- 45 X. Ma, M. Chao and Z. Wang, *Anal. Methods*, 2012, **4**, 1687.
- 46 Y.-R. Kim, S. Bong, Y.-J. Kang, Y. Yang, R. K. Mahajan, J. S. Kim and H. Kim, *Biosens. Bioelectron.*, 2010, **25**, 2366.
- 47 Y. Wang, Y. Li, L. Tang, J. Lu and J. Li, *Electrochem. Commun.*, 2009, **11**, 889.